

Interaction effects on the itinerant ferromagnetism phase transition

Jordi Pera,* Joaquim Casulleras,† and Jordi Boronat‡

Departament de Física, Campus Nord B4-B5, Universitat Politècnica de Catalunya, E-08034 Barcelona, Spain

(Dated: July 22, 2024)

Itinerant ferromagnetism is one of the most studied quantum phase transitions, the transition point and the nature of this phase transition being widely discussed. In dilute Fermi liquids, this analysis has been carried out up to second-order in the gas parameter, where the results for any spin degeneracy are universal in terms of only the s -wave scattering length a_0 . We extend this analysis to third-order where energies depend, not only on a_0 , but also on the s -wave effective range r_0 and the p -wave scattering length a_1 . The introduction in the theory of these new parameters changes the transition point, with respect to the second-order estimation, and also can modify the nature of the phase transition itself. We analyze these interaction effects on the phase transition for different spin values. The emerging phase diagram shows that the type of ferromagnetic transition changes dramatically as a function of r_0 and a_1 and, importantly, that this classification is not solely determined by the spin value, as happens at second order.

I. INTRODUCTION

The Stoner model of itinerant ferromagnetism [1] predicts that a dilute paramagnetic Fermi gas with spin $S = 1/2$ becomes ferromagnetic by increasing the density. At very low density the gas is paramagnetic due to its lower Fermi energy. However, as the density increases, the energy of the non-polarized phase surpasses that of the polarized one, due to the increased interaction effects among particles of different spin. In the polarized phase, interparticle interactions are negligible due to the inhibition of s -wave collisions. The experimental observation of itinerant ferromagnetism in Fermi liquids or gases has been extremely difficult. Ultracold Fermi gases have emerged as one of the best platforms to reach the conditions for this ferromagnetic transition to be observed [2, 3]. However, at large densities the ferromagnetic phase is metastable and competes with the formation of dimers [4]. In fact, there was a first observation of the ferromagnetic transition in cold Fermi gases [5], but the work was revised and finally the authors concluded that the formation of dimers prevented its observation [6]. More recently, it was reported that the ferromagnetic state was effectively observed in a Fermi ${}^7\text{Li}$ gas around a gas parameter $x = k_F a_0 \simeq 1$, with k_F the Fermi momentum and a_0 the s -wave scattering length [7]. On the other hand, this transition has been extensively studied from a theoretical point of view, mainly using quantum Monte Carlo methods [8–15], which agree to localize the ferromagnetic transition around $x \simeq 1$.

Perturbation theory is a well established theoretical tool to study itinerant ferromagnetism. At first order, corresponding to the Hartree-Fock approximation, the celebrated Stoner model [1] predicts a continuous phase transition for $S = 1/2$ and a first-order one for

$S > 1/2$. Following perturbation theory, at second order the Fermi gas suffers a discontinuous transition for any spin value [16]. However, second-order perturbation theory is still not accurate enough as it cannot reproduce Monte Carlo results close to the predicted critical density. In a previous work, the energy as a function of the gas parameter and the spin polarization at third-order has been derived [17]. Unlike second order, a fully analytical expression was not possible to obtain. It is worth noticing that, going beyond second order, universality breaks, meaning that the energy dependence is no longer solely determined by the s -wave scattering length a_0 . Two additional scattering parameters come into play in the description: the s -wave effective range r_0 and the p -wave scattering length a_1 .

In recent years, $\text{SU}(N)$ Fermi gases have been produced experimentally. For example, Ytterbium [18], with spin $5/2$, and Strontium [19], with spin $9/2$, are now available for studying Fermi gases with large spin degeneracy. This relevant achievement has renewed the theoretical interest on these gases. Cazalilla *et al.* [20, 21] showed that Fermi gases made of alkaline atoms, with two electrons in the external shell, such as ${}^{173}\text{Yb}$, present an $\text{SU}(N)$ emergent symmetry. Due to this mathematical property, they argued that the ferromagnetic transition should be a discontinuous one for $S > 1/2$. In Ref. [22], the same authors studied the interaction effects in $\text{SU}(N)$ Fermi gases as a function of the spin degeneracy N . Collective excitations in $\text{SU}(N)$ Fermi gases with tunable spin were also investigated in Ref. [23]. On the other hand, the study of the prethermalization of these systems showed that, under some conditions, the imbalanced initial state could be stabilized for a certain time [24]. Recently, the thermodynamics of ${}^{87}\text{Sr}$, with N that can be tuned up to 10, was analyzed in Ref. [25]. The temperature dependence of itinerant ferromagnetism in $\text{SU}(N)$ Fermi gases, at second order of perturbation theory, has been studied for the first time by Huang and Cazalilla [26]. Once in the fully polarized phase only p -wave scattering is possible. Maki and Enss [27] have studied the shear viscosity and the thermal conductivity of a polarized Fermi gas. More

* jordi.pera@upc.edu

† joaquim.casulleras@upc.edu

‡ jordi.boronat@upc.edu

recently, Bertaina *et al.* [28] reported quantum Monte Carlo calculations of single-component ultracold Fermi gases with p -wave interactions. Finally, and still with single-component Fermi gases, Gao *et al.* [29] established a relationship between the finite-temperature loss rate and the p -wave contact.

In the present work, we explore finite-range effects, defined in terms of the scattering parameters r_0 and a_1 , on the magnetic behavior of a Fermi gas. Our goal is to characterize the ferromagnetic transition for a range of spin values, from $S = 1/2$ to $S = 9/2$, as a function of the above-mentioned scattering parameters. Our results show that the nature of the phase transition is not uniquely defined by the spin value since, depending on the scattering parameters, we can have a continuous transition, a discontinuous one or even no transition at all. This richness contrasts with the prediction made at second-order perturbation theory, where a unique kind of

phase transition (first-order phase transition) was found.

II. PERTURBATIVE SERIES

We study a repulsive Fermi gas at zero temperature, with spin S and spin degeneracy $\nu = 2S + 1$, using perturbation theory. The energy of the gas is a combination of analytic results and numerical estimations. In the very dilute gas regime, only particles with different z -spin component interact via a central potential $V(r)$ (s -wave scattering). The first and second order terms [16] are universal since the energy depends only on the s -wave scattering length. However, going to third order in the gas parameter, we include interactions also between particles of the same z -spin component. The resulting energy involves not only the s -wave scattering length but also the s -wave effective range and the p -wave scattering length [17],

$$\begin{aligned} \frac{E}{N} = & \frac{3}{5}\epsilon_F \left\{ \frac{1}{\nu} \sum_{\lambda} C_{\lambda}^{5/3} + \frac{1}{\nu} \sum_{\lambda} \frac{2}{3\pi} C_{\lambda}^{8/3} (k_F a_1)^3 + \frac{5}{3\nu} \sum_{\lambda_1, \lambda_2} \left[\left(\frac{2}{3\pi} (k_F a_0) C_{\lambda_1} C_{\lambda_2} + \frac{4}{35\pi^2} C_{\lambda_1} C_{\lambda_2} \frac{C_{\lambda_1}^{1/3} + C_{\lambda_2}^{1/3}}{2} F(y) (k_F a_0)^2 \right. \right. \right. \\ & \left. \left. \left. + \frac{1}{10\pi} C_{\lambda_1} C_{\lambda_2} \left(\frac{C_{\lambda_1}^{2/3} + C_{\lambda_2}^{2/3}}{2} \right) \left[\frac{r_0}{a_0} + 2 \frac{a_1^3}{a_0^3} \right] (k_F a_0)^3 + \frac{3}{32\pi^7} [E_3 + E_4 + \sum_{\lambda_3} ((2 - 3\delta_{\lambda_1, \lambda_3} - 3\delta_{\lambda_2, \lambda_3}) E_5)] (k_F a_0)^3 \right] (1 - \delta_{\lambda_1, \lambda_2}) \right\}. \end{aligned} \quad (1)$$

The number of particles in each spin channel is $N_{\lambda} = C_{\lambda} N / \nu$, with N the total number of particles and C_{λ} being the fraction of λ particles (normalized to be one if the system is unpolarized, $N_{\lambda} = N / \nu$, $\forall \lambda$). The Fermi momentum is $k_{F, \lambda} = k_F C_{\lambda}^{1/3}$, k_F being $(6\pi^2 n / \nu)^{1/3}$, and $\epsilon_F = \hbar^2 k_F^2 / 2m$ being the Fermi energy. In Eq. (1), the terms E_3 , E_4 , and E_5 cannot be derived analytically and requires of a numerical integration [17, 30].

Our goal is the description of the ferromagnetic phase transition as a function of the spin and the scattering parameters entering in Eq. (1). The phase diagrams are obtained by minimizing the energy for any value of r_0 and a_1 as a function of the gas parameter $x = k_F a_0$. After this minimization, one can get the polarization P in terms of x . By analyzing this dependence one can study the nature of the transition for each set of scattering parameters. For $S > 1/2$ there is not a single definition of the spin polarization. In our study, we assume that, if the concentration of one species increases, the concentration of all the other species diminish equally.

III. RESULTS

We explore the nature of the phase transition for different values of the p -wave scattering length and s -wave effective range. Given certain values for a_1 and r_0 , we

analyze how the polarization corresponding to the minimum energy changes in terms of the gas parameter. Our results shows a rich variety of different ferromagnetic transitions and even situations where this transition disappears. In Fig. 1, we illustrate these different scenarios. TDT and CT correspond to a total discontinuous (first-order) phase transition and to a continuous (second-order) phase transition, respectively. PDT stands for discontinuous transitions with gaps in the polarization smaller than one. Surprisingly, there can be cases which experience a kind of double transition. First, the polarization increases continuously from 0 to a certain value smaller than 1. And then, a finite jump is observed as if it was a discontinuous transition. These situations are labelled as T2T and P2T. In T2T, after the finite jump, the polarization reaches 1; while in P2T, the polarization is still smaller than 1. The case UCT corresponds to a continuous transition but to states that are not fully polarized, meaning that in these scenarios no itinerant ferromagnetism is possible. The double transitions and the suppression of the ferromagnetic transition are observed only at third-order of perturbation theory. In fact, at second-order the transition is first-order for all values of the spin S [16].

The magnetic susceptibility χ , defined as

$$\frac{1}{\chi} = \frac{1}{n} \left(\frac{\partial^2 (E/N)}{\partial P^2} \right)_x, \quad (2)$$

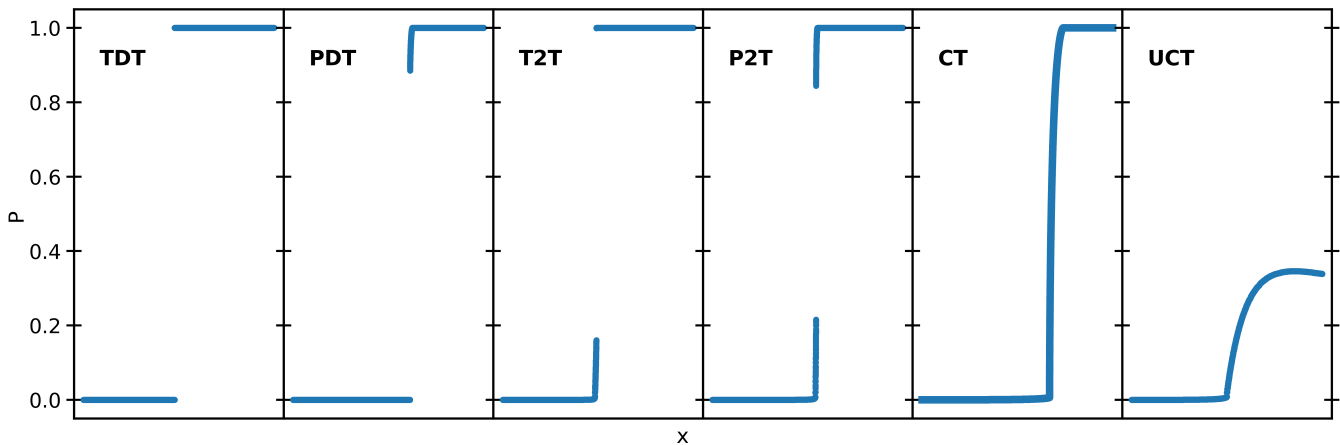


FIG. 1: Main types of phase transitions using the polarization P as order parameter. From left to right, discontinuous, double and continuous.

can be obtained from the energy (1). In Fig. 2, we show characteristic results of χ around the transition point for the main types of behaviors: double, discontinuous, and continuous. The location of the peaks indicates the transition points, their height being finite and infinite for the discontinuous and continuous case, respectively.

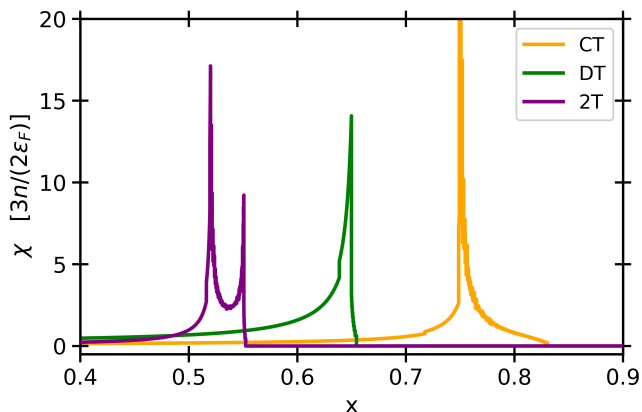


FIG. 2: Magnetic susceptibilities at the phase transition. From left to right: double, discontinuous, and continuous transitions. Notice that the continuous one diverges at the transition point.

In Fig. 3, we show the different types of phase transition for $S = 1/2$ as a function of r_0 and a_1 . We selected a range of values for r_0 and a_1 where the diagram is outstanding. With different colors, and the acronyms discussed above, we can easily identify the different regimes. As one can see, the dominant transition is a continuous one. However, for small and negative r_0 values there are discontinuous transitions. And also, if r_0 is large and negative or a_1 is large, there is no transition at all (NT), i.e., the Fermi gas remains unpolarized for any value of the gas parameter. We point out that, if p -wave inter-

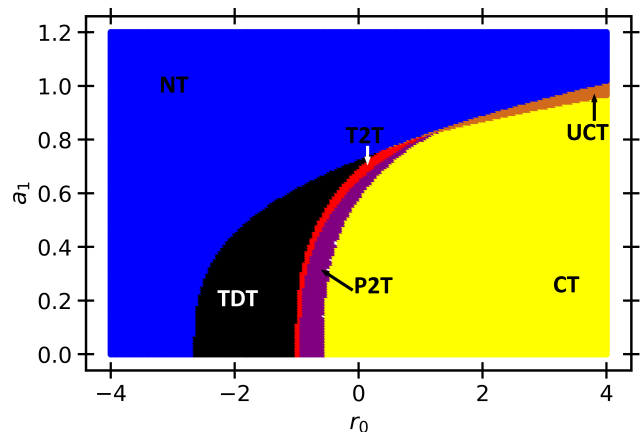


FIG. 3: Ferromagnetic phase transition types for $S = 1/2$.

actions between particles of same spin are included, the hard-spheres case ($r_0 = 2/3$ and $a_1 = a_0$) falls into this latter case.

Once we increase the spin degeneracy, we continue to observe different scenarios. Our results for $S = 3/2, 5/2, 7/2,$ and $9/2$ are shown in Fig. 4. The most relevant difference between $S = 1/2$ and $S > 1/2$ is that the types of phase transitions are distributed oppositely. In spin $1/2$, we have continuous transitions for positive r_0 and the discontinuous ones appear for negative r_0 values. Now, for larger spin, the situation is reversed. The continuous transitions happen for negatives or small r_0 , and the discontinuous ones for large values of r_0 . As before, if a_1 is large enough, there is no transition at all. Therefore, at third order of perturbation theory the value of the spin does not determine the phase transition type, similarly to the case of $S = 1/2$.

There is one specific case which has been studied using diffusion Monte Carlo (DMC) [9] that we want to high-

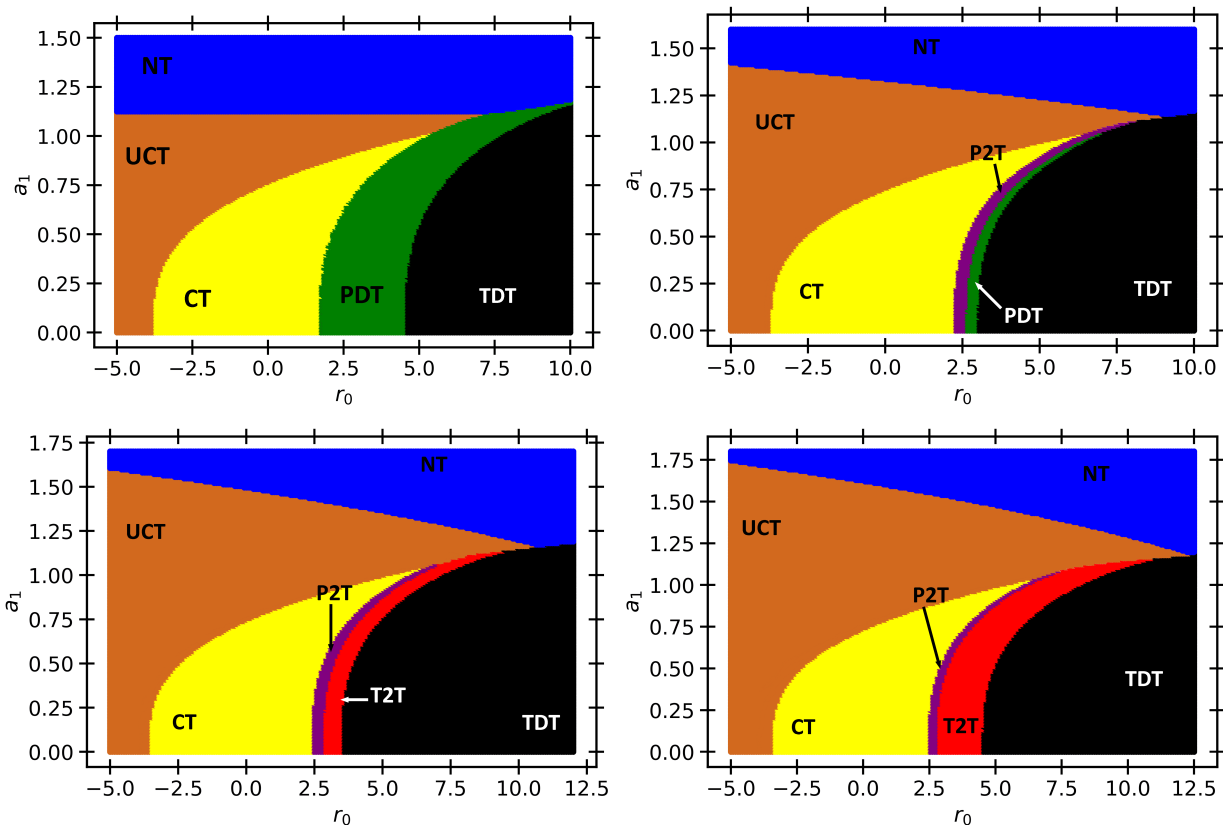


FIG. 4: Ferromagnetic phase transition types for $S = 3/2, 5/2, 7/2,$ and $9/2$ (from left to right and from top to bottom).

light. In those calculations, a hard-sphere potential was considered ($r_0 = 2a_0/3$ and $a_1 = a_0$), but the p -wave interaction effects between particles of same spin were neglected. If we look at Eq. (1), the neglected term is the second one in the formula, that is,

$$\frac{1}{\nu} \sum_{\lambda} \frac{2}{3\pi} C_{\lambda}^{8/3} (k_F a_1)^3. \quad (3)$$

To translate this case into our formalism, one can redefine the effective range as $\bar{r}_0/a_0 = (r_0/a_0 + 2a_1^3/a_0^3)$. In practice, it means to follow the line $a_1 = 0$ with \bar{r}_0 in Figs. 3 and 4. For the hard-sphere potential, $\bar{r}_0/a_0 = 2/3 + 2 \approx 2.67$. Around this region, we have partial discontinuous transitions for $S = 3/2$ and $5/2$. And, although it is hard to see, for $S = 7/2$ and $9/2$, there are partial double transitions. This particular case has been analyzed in Ref. [16].

IV. LANDAU THEORY

Landau theory of phase transitions helps to understand the origin of the different transition types observed in our study and the location of the critical points. According to the order of our approximation, the parameters of the

Landau expansion depend on x up to third order. It is written as an expansion in terms of the polarization P ,

$$f(x, P) - f_0(x) = -\frac{A}{2}(\bar{x}(x) - x_0)P^2 - \frac{B(x)}{3}|P|^3 + \frac{C(x)}{4}P^4 + \frac{L(x)}{4}P^4 \ln|P|, \quad (4)$$

with $f(x, P) = 5E/(3N\epsilon_F)$ and $x_0 = \pi/2$. The coefficients in Eq. (4) depend on the gas parameter x through an involved expression (see Appendix A). Although it is not shown here, we point out that the parameter L is the only *universal* one since it does not depend on r_0 and a_1 . For the sake of simplicity, from now on, we will not specify that the coefficients of Eq. (4) depend on the gas parameter x . In order to determine the transition point, one imposes two conditions: *i*) the energy has to be a minimum, that is, its first derivative must be zero, and *ii*) the energy must be smaller than the unpolarized phase energy, to have a global minimum. One solution to these criteria is $P^* = 0$ and $\bar{x}(x) = x_0$, which would represent a continuous transition. However, there are other solutions.

The other solutions, that give rise to discontinuous

transitions, satisfy the following equations,

$$\ln |P^*| = -\left(\frac{1}{2} + \frac{C}{L}\right) + \frac{2B}{3L|P^*|}, \quad (5)$$

$$\bar{x}^* = x_0 - \frac{B}{3A}|P^*| - \frac{L}{4A}|P^*|^2. \quad (6)$$

We rewrite Eq. (5) to better explore the range where a solution exists,

$$\frac{\alpha}{|P^*|} - \ln |P^*| = \beta, \quad (7)$$

with $\alpha = 2B/(3L)$ and $\beta = 1/2 + C/L$. There are three domains in which we find a solution: a) if $\alpha \geq 0, \beta \geq \alpha$; b) if $\alpha \in (-1, 0), \beta \leq -1 - \ln(-\alpha)$; and c) if $\alpha \leq -1, \beta \leq \alpha$.

We first analyze $S = 1/2$, as it is the most relevant case. For this spin value, $B = 0$, and hence, $\alpha = 0$ too. If there is no logarithmic term ($L = 0$) and $C > 0$ (case that corresponds to the Stoner model [1]), the Fermi gas shows a continuous transition. However, if a logarithmic term with a positive coefficient ($L > 0$) is present, then a discontinuous transition occurs; this is what happens when we expand the energy up to second order in the gas parameter [16]. In the present case, we need to analyze the shape of L , which is universal, and the effects of r_0 and a_1 on the other parameters in Eq. (4).

As an example, we plot in Fig. (5) the case exposed at the end of Sec. III, that is, $r_0 \approx 2.67$ and $a_1 = 0$. We see that the parameter C is positive whereas L changes its sign. At low values of the gas parameter, L is positive making a discontinuous transition possible. While x grows, it becomes negative, implying a continuous transition. In fact, for a discontinuous transition to exist, it is necessary that Eqs. (5) and (6) are satisfied before L changes sign. It turns out that there is no solution in this regime, hence, one finds a critical point $x^* = 0.868$ for a continuous transition with $\bar{x}(x) = x_0$. Summarizing, the transition is continuous, because L has become negative, eliminating the point of inflection in the energy that could cause a discontinuous one.

Landau theory also helps to understand the regime where a phase transition does not occur, that is, the region depicted in blue in Figs. 3 and 4. In this regime, the shape of the parameters is very similar to the ones presented in Fig. 5, except for $\bar{x}(x) - x_0$. In Fig. 6, we show $\bar{x}(x) - x_0$ for $r_0 = -5$ and $a_1 = 0$, a set of values for which there is no transition. We can see that that the function $\bar{x}(x) - x_0$ does not cross zero, and hence, there is no solution that can give us a transition.

This approach shows also some limitations. Coming back to Fig. 3, one can see that there is a region featuring discontinuous transitions when r_0 is negative. In principle, the Landau model could be applicable in such cases, because, with negative r_0 , C may become also negative, and then we could have a positive value for β after

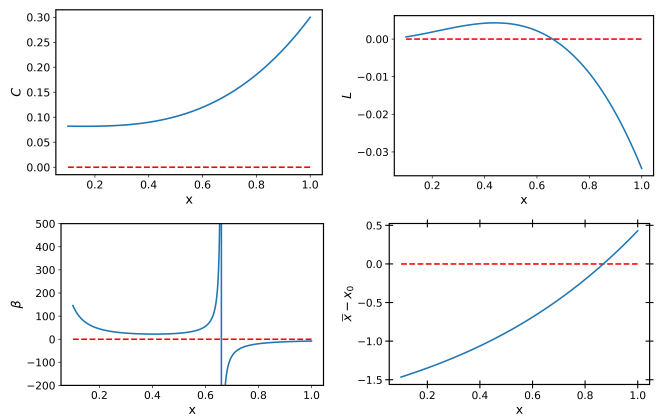


FIG. 5: Parameters C , L , β , and $\bar{x}(x) - x_0$ in terms of the gas parameter for $S = 1/2$, $r_0 = 2 + 2/3$ and $a_1 = 0$.

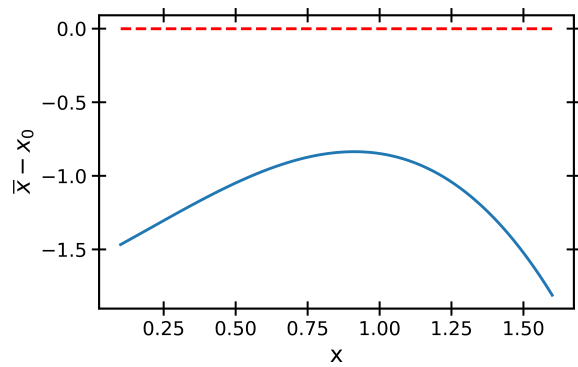


FIG. 6: $\bar{x}(x) - x_0$ in terms of the gas parameter for $S = 1/2$, $r_0 = -5$ and $a_1 = 0$.

L changes sign, hence predicting a discontinuous transition. However, C becomes negative for a very large value of r_0 which is far from the results shown in Fig. 3. Therefore, the Landau expansion is only accurate when we deal with continuous transitions. This is an expected result since the Taylor expansion underlying the theory works effectively for $P \lesssim 0.5$.

In the following, we analyze the case of $S > 1/2$. In this case, the key point is to understand the regime of a continuous transition since this is unexpected, as there is a cubic term in the Landau expansion which would lead to a discontinuous transition. If instead one observes a continuous scenario, it must be the result of a cancellation between the P^3 and $P^4 \ln |P|$ terms. In Fig. 7, we show L , which is universal. For $S = 1/2$, the sign of L is the key to understand what is happening as it caused the change of sign of β . Now, for large S , we see that it is positive everywhere, hence, the origin of the different transitions must come either from B or C .

In Fig. 8, we show the parameters B and C for two situations. The plots in the left correspond to the continuous region (yellow) of Fig. 4, that is with $r_0 = 0$ and $a_1 = 0$. And the plots in the right stand for the discontinuous

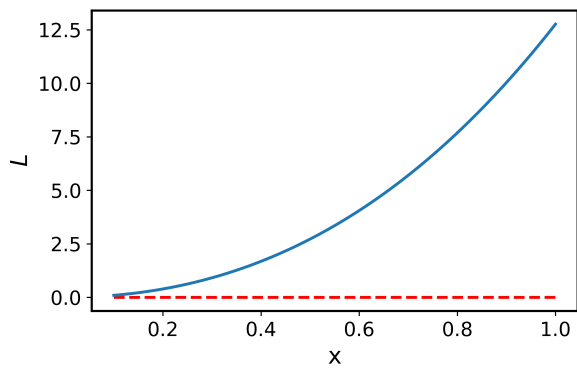


FIG. 7: L in terms of the gas parameter for $S = 5/2$.

region (black) of Fig. 4, that is with $r_0 = 5$ and $a_1 = 0$. In the first case ($r_0 = 0$) the critical point is at $x = 0.63$, and in the second one ($r_0 = 0.5$) at $x = 0.666$, according to Landau theory. For those critical values, C is positive for both situations. However, in the first scenario, B is negative because it changes sign before reaching a value of 0.6, but, in the second one, B is positive because the change of sign happens after a value of 0.7.

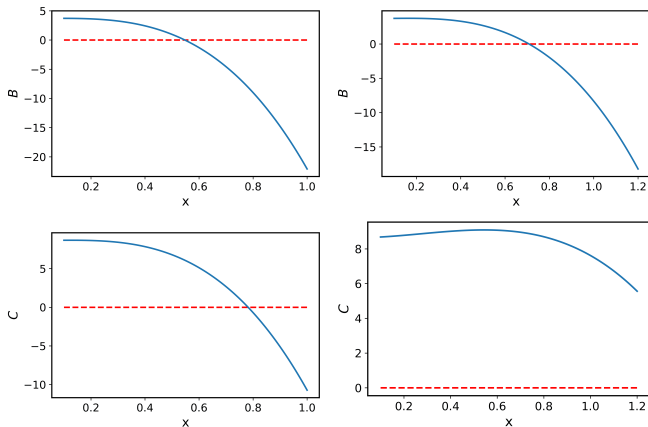


FIG. 8: B (top) and C (bottom) for $S = 5/2$. The left figures have $r_0 = 0$ and the right ones $r_0 = 5$. All of them have $a_1 = 0$.

So, in the case $r_0 = 0$, at the transition point, β is positive because both L and C are positive, but, α is negative because B has changed sign. This can be seen in Fig. 9. Therefore, according to the conditions stated above, the discontinuous transition is not possible. Landau theory for this case concludes that the change of sign of B allows a continuous transition to happen at spin values larger than $1/2$. The expected overall negative sign in the cubic term P^3 is what lead to believe that the transition would be always discontinuous. But here, we are seeing that B can change sign, and make the overall sign of the cubic term positive, eliminating the inflection in the energy, and hence, giving rise to a continuous transition. In the second scenario ($r_0 = 5$), at the transition point,

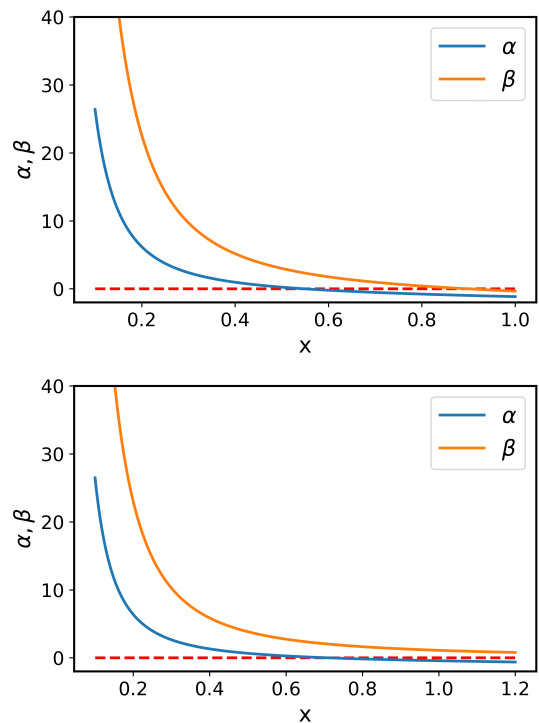


FIG. 9: Comparison of α and β in terms of x for $r_0 = 0$ (top) and $r_0 = 5$ (bottom). Both cases stand for $S = 5/2$ and $a_1 = 0$.

everything is positive: B , C , L , α , and β (see Fig. 9). Therefore, as β is larger than α a discontinuous transition emerges, in agreement with perturbation theory. Essentially, this is the expected case in which the overall sign of the cubic term is negative, causing an inflection in the energy and making the transition discontinuous.

V. SUMMARY AND CONCLUSIONS

We have studied the itinerant ferromagnetism phase transition of Fermi gases as a function of the s -wave effective range and p -wave scattering length within perturbation theory to third order in the gas parameter [17]. The results presented stand for gases with $S = 1/2, 3/2, 5/2, 7/2$ and $9/2$. We recall that electrons have $S = 1/2$, Ytterbium has $S = 5/2$, and Strontium has $9/2$.

The nature of this phase transition has been discussed for a long time. First, the Stoner model [1] predicted a continuous transition for $S = 1/2$, and a discontinuous one for the rest. Later, a second-order model predicted that all the transitions are discontinuous, independently of the spin value [16]. At third order, the description changes again: any Fermi gas, independently of its spin, can have any kind of transition. It does not matter the spin value, we can either have a continuous transition, a discontinuous one, or even no transition at all. Perhaps, the more striking result is that there can be continuous

transitions for $S > 1/2$ [17]. Up to now, it was well established that for $S > 1/2$ the transition would be discontinuous, and the main discussion happened around the $S = 1/2$ case.

Our results show that for $S = 1/2$, the dominant transition is the continuous one, which happens mostly for positive values of r_0 . However, there exists a small region for negative values of r_0 where the discontinuous transitions emerge. On the contrary, for $S > 1/2$, this situation is reversed. For positive values of r_0 , we encounter first-order phase transitions, while for negative and small values of r_0 , Fermi gases suffer a second-order phase transition. In order to understand this variability, we have used Landau theory. For $S > 1/2$, we show why there can be a continuous transition for low values of r_0 , and also explain the discontinuous regime. For $S = 1/2$, the continuous behavior has been explained, however, Landau theory has failed to account for the discontinuous solutions.

Incorporating the two additional scattering parameters has enriched the itinerant ferromagnetism scenario. Should someone delve deeper into perturbation theory and provide additional detail and information regarding the potential, we anticipate not a decrease of this rich variability, but rather a modification of the domains where different phase transitions emerge.

VI. ACKNOWLEDGMENTS

We acknowledge financial support from Ministerio de Ciencia e Innovación MCIN/AEI/10.13039/501100011033 (Spain) under Grant No. PID2020-113565GB-C21 and from AGAUR-Generalitat de Catalunya Grant No. 2021-SGR-01411.

Appendix A: Parameters of the Landau expansion

In this section we show the expression for all the parameters of the Landau expansion in terms of the gas degeneracy ($\nu = 2s + 1$) and the gas parameter ($x = k_F a_0$). We first show the Landau expansion up to fourth order in P including the logarithmic term that comes from the second order term in perturbation theory,

$$f(x, P) - f_0(x) = -\frac{A}{2}(\bar{x} - x_0)P^2 - \frac{B(x)}{3}|P|^3 + \frac{C(x)}{4}P^4 + \frac{L(x)}{4}P^4 \ln |P|. \quad (\text{A1})$$

The parameters that are invariant in any order are

$$f(x, P) = \frac{5E}{3N\epsilon_F}, \quad A = \frac{20}{9\pi}(\nu - 1), \quad \text{and} \quad x_0 = \pi/2. \quad (\text{A2})$$

We will start with the constant term with respect to P ,

$$f_0(x) = 1 + \frac{10}{9\pi}(\nu - 1)x + \frac{4}{21\pi^2}(\nu - 1)(11 - 2 \ln 2)x^2 + \frac{1}{6\pi}(\nu - 1)x_0x^2 + \frac{1}{3\pi}(\nu + 1)x_1^3 + (\nu - 1)[0.125964142 + 0.095637082(\nu - 3)]x^3, \quad (\text{A3})$$

with $x_1 = k_F a_1$.

Then, the modified x we have called \bar{x} ,

$$\bar{x} = x + \frac{2}{15\pi}(22 - 7\nu + 4(\nu - 1) \ln 2)x^2 - \frac{\nu - 4}{12}x_0x^2 - \frac{\nu + 4}{6}x_1^3 - \frac{9\pi}{10}(0.355828883 - 0.139542655\nu - 0.027888923\nu^2)x^3. \quad (\text{A4})$$

The next parameter is the one of $|P|^3$, we notice that this term is zero if $\nu = 2$,

$$B(x) = \frac{5}{27}(\nu - 1)(\nu - 2) + \frac{2}{81\pi^2}(\nu - 1)(\nu - 2)(44 + \nu + 8(\nu - 1) \ln 2)x^2 + \frac{5(\nu - 1)(\nu - 2)(\nu + 8)}{162\pi}x_0x^2 \\ + \frac{(\nu - 1)(\nu - 2)(5\nu - 40)}{81\pi}x_1^3 - 3(\nu - 1)(\nu - 2)(0.086700582 + 0.016099453\nu + 0.008647721\nu^2)x^3. \quad (\text{A5})$$

Now, the term of P^4 ,

$$C(x) = \frac{20}{243}(\nu - 1)(\nu^2 - 3\nu + 3) + (\nu - 1)\frac{528 - 336\nu - 16\nu^2 + 29\nu^3 - (96 - 192\nu + 128\nu^2 - 32\nu^3) \ln 2}{729\pi^2}x^2 \\ + \frac{20\nu^3}{243\pi^2}(\nu - 1) \ln \frac{\nu}{6}x^2 + \frac{10}{729\pi}(\nu - 1)(\nu + 2)(\nu^2 - 3\nu + 3)x_0x^2 + \frac{20}{729\pi}(\nu - 1)(\nu - 2)(\nu^2 - 3\nu + 3)x_1^3 + \\ + 4(\nu - 1)[0.114687364 - 0.043172957\nu + 0.006693296\nu^2 + 0.007873117\nu^3 - 0.002568852\nu^4 \\ - (0.005175610 - 0.001007688\nu)\nu^3 \ln \nu]x^3. \quad (\text{A6})$$

And finally, the parameter of the logarithmic term,

$$L(x) = \frac{20\nu^3}{243\pi^2}(\nu - 1)x^2 - 4(\nu - 1)\nu^3(0.005175610 - 0.001007688\nu)x^3. \quad (\text{A7})$$

-
-
- [1] E. C. Stoner, Lxxx. atomic moments in ferromagnetic metals and alloys with non-ferromagnetic elements, The London, Edinburgh, and Dublin Philosophical Magazine and Journal of Science **15**, 1018 (1933).
- [2] C. Pfeleiderer, S. Julian, and G. Lonzarich, Non-Fermi-liquid nature of the normal state of itinerant-electron ferromagnets, Nature **414**, 427 (2001).
- [3] M. Leduc, Spin Polarized Helium-3, a Playground in Many Domains of Physics, J. Phys. Colloq. **51**, 317 (1990).
- [4] Y. Ji, G. L. Schumacher, G. G. T. Assumpç ao, J. Chen, J. T. Mäkinen, F. J. Vivanco, and N. Navon, Stability of the repulsive Fermi gas with contact interactions, Phys. Rev. Lett. **129**, 203402 (2022).
- [5] G.-B. Jo, Y.-R. Lee, J.-H. Choi, C. A. Christensen, T. H. Kim, J. H. Thywissen, D. E. Pritchard, and W. Ketterle, Itinerant ferromagnetism in a Fermi gas of ultracold atoms, Science **325**, 1521 (2009).

- [6] C. Sanner, E. J. Su, W. Huang, A. Keshet, J. Gillen, and W. Ketterle, Correlations and pair formation in a repulsively interacting Fermi gas, *Phys. Rev. Lett.* **108**, 240404 (2012).
- [7] G. Valtolina, F. Scazza, A. Amico, A. Burchianti, A. Recati, T. Enss, and M. Inguscio, Exploring the ferromagnetic behaviour of a repulsive Fermi gas through spin dynamics, *Nature Phys.* **13**, 704–709 (2017).
- [8] G. J. Conduit, A. G. Green, and B. D. Simons, Inhomogeneous phase formation on the border of itinerant ferromagnetism, *Phys. Rev. Lett.* **103**, 207201 (2009).
- [9] S. Pilati, G. Bertaina, S. Giorgini, and M. Troyer, Itinerant ferromagnetism of a repulsive atomic Fermi gas: A quantum Monte Carlo study, *Phys. Rev. Lett.* **105**, 030405 (2010).
- [10] S.-Y. Chang, M. Randeria, and N. Trivedi, Ferromagnetism in the upper branch of the feshbach resonance and the hard-sphere Fermi gas, *Proceedings of the National Academy of Sciences* **108**, 51 (2011).
- [11] G. J. Conduit and B. D. Simons, Itinerant ferromagnetism in an atomic Fermi gas: Influence of population imbalance, *Phys. Rev. A* **79**, 053606 (2009).
- [12] P. Massignan, Z. Yu, and G. M. Bruun, Itinerant ferromagnetism in a polarized two-component Fermi gas, *Phys. Rev. Lett.* **110**, 230401 (2013).
- [13] X. Cui and H. Zhai, Stability of a fully magnetized ferromagnetic state in repulsively interacting ultracold Fermi gases, *Phys. Rev. A* **81**, 041602 (2010).
- [14] F. Arias de Saavedra, F. Mazzanti, J. Boronat, and A. Polls, Ferromagnetic transition of a two-component Fermi gas of hard spheres, *Phys. Rev. A* **85**, 033615 (2012).
- [15] S. Pilati, G. Orso, and G. Bertaina, Quantum monte carlo simulations of two-dimensional repulsive Fermi gases with population imbalance, *Phys. Rev. A* **103**, 063314 (2021).
- [16] J. Pera, J. Casulleras, and J. Boronat, Itinerant ferromagnetism in dilute SU(N) Fermi gases, *SciPost Phys.* **14**, 038 (2023).
- [17] J. Pera, J. Casulleras, and J. Boronat, Beyond universality in repulsive SU(N) fermi gases (2024), arXiv:2206.06932 [cond-mat.quant-gas, to appear in *SciPost Phys.*].
- [18] G. Pagano, M. Mancini, G. Cappellini, P. Lombardi, F. Schäfer, H. Hu, X. J. Liu, J. Catani, C. Sias, M. Inguscio, and L. Fallani, A one-dimensional liquid of fermions with tunable spin, *Nature Phys.* **10**, 198–201 (2014).
- [19] A. Goban, R. B. Hutson, G. E. Marti, S. L. Campbell, M. A. Perlin, P. S. Julienne, J. P. D’Incao, A. M. Rey, and J. Ye, Emergence of multi-body interactions in a fermionic lattice clock, *Nature (London)* **563**, 369–373 (2018).
- [20] M. A. Cazalilla, A. F. Ho, and M. Ueda, Ultracold gases of ytterbium: ferromagnetism and mott states in an SU(6) fermi system, *New Journal of Physics* **11**, 103033 (2009).
- [21] M. A. Cazalilla and A. M. Rey, Ultracold fermi gases with emergent su(n) symmetry, *Reports on Progress in Physics* **77**, 124401 (2014).
- [22] S. Xu, J. T. Barreiro, Y. Wang, and C. Wu, Interaction effects with varying n in SU(n) symmetric fermion lattice systems, *Phys. Rev. Lett.* **121**, 167205 (2018).
- [23] C. He, Z. Ren, B. Song, E. Zhao, J. Lee, Y.-C. Zhang, S. Zhang, and G.-B. Jo, Collective excitations in two-dimensional su(n) fermi gases with tunable spin, *Phys. Rev. Res.* **2**, 012028 (2020).
- [24] C.-H. Huang, Y. Takasu, Y. Takahashi, and M. A. Cazalilla, Suppression and control of prethermalization in multicomponent Fermi gases following a quantum quench, *Phys. Rev. A* **101**, 053620 (2020).
- [25] L. Sonderhouse, C. Sanner, R. B. Hutson, A. Goban, T. Bilitewski, L. Yan, W. R. Milner, A. M. Rey, and J. Ye, Thermodynamics of a deeply degenerate su(n)-symmetric Fermi gas, *Nat. Phys.* **16**, 1216–1221 (2020).
- [26] C.-H. Huang and M. A. Cazalilla, Itinerant ferromagnetism in su(n)-symmetric fermi gases at finite temperature: First order phase transitions and time-reversal symmetry (2023), arXiv:2211.12882 [cond-mat.quant-gas].
- [27] J. Maki and T. Enss, Transport in p -wave-interacting Fermi gases, *Phys. Rev. A* **107**, 023317 (2023).
- [28] G. Bertaina, M. G. Tarallo, and S. Pilati, Quantum monte carlo study of the role of p -wave interactions in ultracold repulsive Fermi gases, *Phys. Rev. A* **107**, 053305 (2023).
- [29] X.-Y. Gao, D. Blume, and Y. Yan, Temperature-dependent contact of weakly interacting single-component Fermi gases and loss rate of degenerate polar molecules, *Phys. Rev. Lett.* **131**, 043401 (2023).
- [30] R. Bishop, Ground-state energy of a dilute Fermi gas, *Annals of Physics* **77**, 106 (1973).